



## Addressing personalized thermal comfort in residential settings: A novel dual-supply vent air conditioner

Yuxin Yang <sup>a</sup>, Zisheng Zhao <sup>b</sup>, Junmeng Lyu <sup>a</sup>, Bo Wang <sup>b</sup>, Jinbo Li <sup>b</sup>,  
Shuguang Zhang <sup>b</sup>, Zhiwei Lian <sup>a,\*</sup>

<sup>a</sup> School of Design, Shanghai Jiao Tong University, Shanghai, 200240, China

<sup>b</sup> Guangdong Midea Air-Conditioning Equipment Co., Ltd, Guangdong, 528311, China



### ARTICLE INFO

#### Keywords:

Simulation  
Thermal comfort  
Air distribution  
Multiple thermal zones  
Air conditioner

### ABSTRACT

A new approach was proposed for meeting diverse thermal comfort demands of different occupants by using a dual-supply vent air conditioner with independent control of the air supply parameters at each vent to establish distinct thermal environments. The feasibility of this method was tested in a living room environment, and numerical simulation was conducted to explore the differences in thermal environment at various locations under different air supply temperatures, velocities, directions, and vent positions. The results indicated that, within the targeted air supply zone, the maximum temperature difference could reach around 2.5 °C. Considering the Cooling Effect of air velocity, the maximum Equivalent Temperature difference was around 4.5 °C, which could address the differences in common personalized thermal comfort preference. Utilizing the differential air supply velocities of different vents was an effective means of achieving diverse thermal environments, although attention should be paid to local thermal discomfort caused by drafts. This approach may offer a new perspective in addressing the differing thermal comfort preferences among occupants within the same residential room, additionally providing innovative insights for improving traditional air conditioning systems.

### Nomenclature

D	Air supply direction (°)
d	Distance between two inlets (m)
t	Air supply temperature (°C)
T <sub>a</sub>	Air temperature (°C)
V	Air supply velocity (m/s)
V <sub>a</sub>	Air velocity (m/s)

### Abbreviation

CE	Cooling effect (°C)
CFD	Computational fluid dynamics
EqT	Equivalent temperature (°C)

\* Corresponding author.

E-mail address: [zwlian@sjtu.edu.cn](mailto:zwlian@sjtu.edu.cn) (Z. Lian).

PMV	Predicted mean vote
SET	Standard effective temperature (°C)
DR	Draught Rate (%)
PD	Percentage of Dissatisfied due to vertical temperature differences (%)

## 1. Introduction

In order to improve the thermal comfort in air-conditioned spaces, the temperature setpoint, air distribution method, and other aspects of the air conditioner have been thoroughly studied [1,2]. However, traditional central air conditioning systems or split air conditioners are usually designed to maintain a uniform thermal environment throughout the occupied zone [3]. Due to individual differences in thermal environment, such a single-parameter environment cannot satisfy everyone simultaneously [4]. Therefore, the establishment of diverse thermal environments is necessary to further improve the overall satisfaction rate with the thermal conditions.

Personalized differences in thermal comfort demands stem from various factors, including gender [5,6], age [7–9] metabolic rate, BMI [10], as well as variations in clothing insulation and activity levels, etc. Numerous studies have indicated that females, influenced by factors such as clothing behavior [11] and lower Resting Metabolic Rate [12], exhibit heightened sensitivity to the thermal environment [13] and may prefer higher temperatures. The quantification of these differences has also been thoroughly examined. Lan et al. conducted experimental research on gender-based variations in comfortable temperature among Chinese individuals, revealing that the comfortable operative temperature for females is approximately 1 °C higher than that for males [14]. In a study on Indian office buildings, Indraganti et al. found that comfortable temperatures for females, the young, and individuals with low body mass index were higher compared to their male, elderly, and obese counterparts, respectively, with differences ranging from 0.3 to 1.0 °C [10].

In recent years, there has been a flourishing development in the field of technological research aimed at addressing personalized thermal comfort demands [15], with developments including contact-based heated or cooled chairs [16], foot warmers, and leg warmers [17]. A substantial amount of research has also delved into harnessing the potential of using fans or personal ventilation to create specific thermal environments and its role in improving thermal comfort and energy efficiency [18–21]. Similarly, it can be used as a solution for localized thermal comfort needs or differentiated thermal comfort needs, Lyu et al. explored the potential of different combinations of air temperature and velocity in addressing gender differences in thermal comfort [22]. Rissetto et al. concluded that "use of a personalized ceiling fan could compensate for inter- and intrapersonal differences in thermal requirements" [18]. These studies all demonstrated that changing the local air velocity was an effective means of improving local thermal comfort. However, the introduction of contact-based systems or fans faces challenges due to complex installation or spatial constraints [23].

Theoretically the air conditioner can also regulate local air velocity and temperature, so directly utilizing air conditioners to create multiple thermal environments within a single room may offer more flexibility in various application scenarios, making it a promising

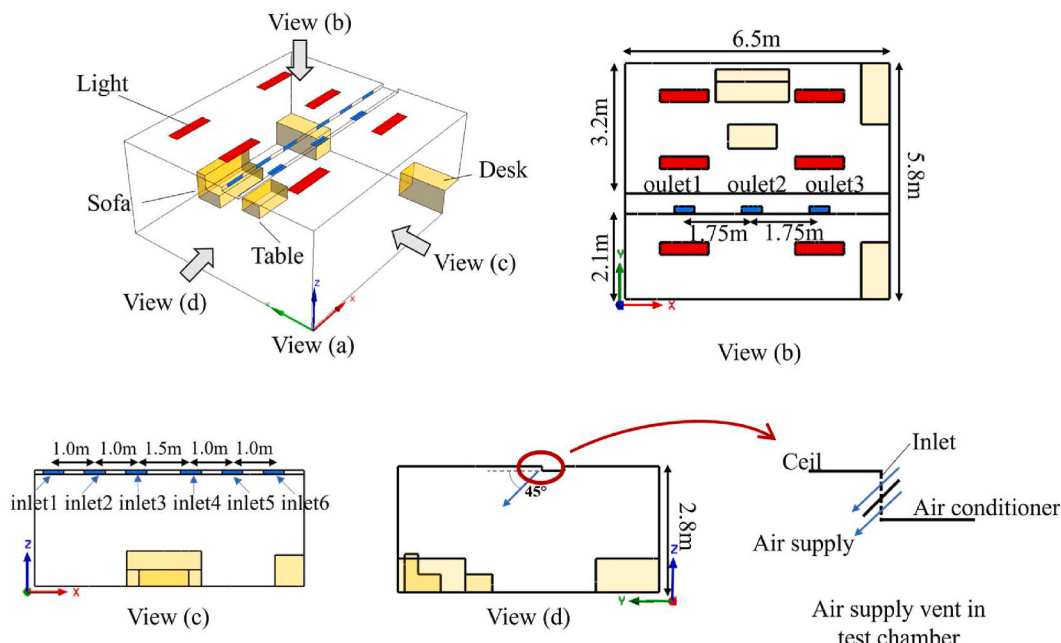


Fig. 1. Schematic representation of the scenario.

approach to address variations in personalized thermal comfort. The control of localized temperatures through air conditioning has been demonstrated by Liu et al. and Shao et al., who utilized multiple air inlets with different parameters based on stratified ventilation to establish distinct thermal environments within classrooms [24,25]. The feasibility of this operation was well documented by studies on the zonal control of thermal environments by differentiated air supply from multiple air outlets in some larger shared spaces [26–28]. Some studies have also explored the effectiveness of passively exploiting environmental inhomogeneity to meet individual thermal differences in the environment with single air supply parameters [29,30]. However, exploration on zonal control of air conditioning in small shared spaces such as living rooms is still limited.

Considering the aforementioned factors, there is a lack of research exploring the possibility of using multi-vent air conditioners for differentiated thermal environment creation in small shared spaces such as living rooms. Meanwhile, there has also been limited research considering the use of air velocity field differences of domestic air conditioners to create differentiated thermal environments based on air supply temperature differences. So, this study proposes an innovative approach using two independently controlled air supply vents on a single air conditioner to establish diverse thermal zones within a living room. The primary objectives are twofold: (1) Evaluate the effectiveness of using only an air conditioner to establish diverse thermal environments within residential rooms, addressing general differences in personalized thermal preferences while mitigating localized discomfort, and (2) analyzed the impact of air supply parameters on air temperature and velocity distribution, as well as their combined effects on thermal sensation. This study is expected to provide new insights into addressing personalized thermal comfort demands in residential settings.

## 2. Methodology

### 2.1. Experiments

#### 2.1.1. Test chamber

The experiments were conducted within a test chamber at Shanghai Jiao Tong University in October, as illustrated in Fig. 1. The room's dimensions were 6.5 m (x) × 5.8 m (y) × 2.8 m (z). In the test chamber, as shown in Fig. 1, two air conditioner terminals were installed on the ceiling. Specifically, only inlet2 and inlet5 were physically present within the test chamber, both exhibiting dimensions of 0.5 m (x) × 0.1 m (z). The return air outlets, with dimensions of 0.5 m (x) × 0.2 m (y), were located on the ceiling. For the experiment, outlet 1 and outlet 3 were utilized, while the remaining vents were reserved for the numerical simulation setup. The experimental and simulated air vents were used to imitate the general domestic air-conditioning terminal, the specific outlook of the application can be referred to Fig. 18. Six lights, each with a heat load of 36W, were distributed on the ceiling. To replicate a typical living room arrangement, the room included a sofa, a table, and two desks.

Given that the primary objective of this study is to investigate the thermal environment differences caused by differentiated air supply, the test chamber was with exterior walls on almost all sides and minimal direct sunlight exposure. This was done to maintain as uniform wall temperatures as possible and mitigate the impact of temperature variations on indoor temperature distribution. Throughout the simulation process, the influence of temperature differences in exterior walls on the environment was avoided by setting the wall temperature same.

The summarized information of the measuring instruments is presented in Table 1. Throughout the experimental process, the indoor relative humidity was  $53 \pm 3\%$  and Black globe temperature was  $26.4 \pm 0.2^\circ\text{C}$ .

#### 2.1.2. Test procedure

The measurements were conducted under stable conditions, with nine vertical measurement lines strategically placed within the room. At heights of 0.1 m, 0.6 m, 1.1 m, 1.6 m, 2.1 m, and at the heights of 2.6 m in Line-2 and Line-8 close to the air supply inlets, air temperature and air velocity were monitored. The coordinates of the measurement lines were as follows: Line-1 (1.5, 4.3), Line-2 (1.5, 2.8), Line-3 (1.5, 1.3), Line-4 (3.5, 4.3), Line-5 (3.5, 2.8), Line-6 (3.5, 1.3), Line-7 (4.8, 4.3), Line-8 (4.8, 2.8), and Line-9 (4.8, 1.3), which were uniformly distributed throughout the room. SWEMA omnidirectional anemometer systems were used to measure air temperature and velocity along the nine sampling lines (Line-1~Line-9). The measurement time for each sampling line was 10 min and the sampling interval was 0.1s. After the completion of measurement of one sampling line, the measuring rod was moved to the next position. New sampling began after a 10-min interval to ensure the stability of the flow field.

## 2.2. Numerical simulation

### 2.2.1. Numerical simulation approach

ANSYS SpaceClaim 2022 R1 and Workbench 2022 R1 Mesh were employed for the construction of the geometric model and mesh generation, respectively. ANSYS Fluent 2022 R1 was utilized for the calculation of the indoor airflow field. The building envelope consisted of the ceiling, walls, and floor, all of which were considered to be constant temperature walls [31]. The temperature settings

**Table 1**  
Information on measurement tools.

Measured parameter	Instrument	Range	Accuracy
Air temperature	Swema 03+, SWEMA AB, Sweden	10–40 °C	$\pm 0.2^\circ\text{C}$
Air velocity	Swema 03+, SWEMA AB, Sweden	0–10 m/s	$\pm 0.01 \text{ m/s}$
Relative humidity	TR-76Ui, T&D CO., Japan	10–95%	$\pm 5\%$
Wall surface temperature	FLUKE 62 max+; A Fluke Company, USA	-30–650 °C	$\pm 1.0^\circ\text{C}$ or $\pm 1.0\%$ of reading, whichever is greater
Black globe temperature	Swema 05, SWEMA AB, Sweden	0–50 °C	$\pm 0.1^\circ\text{C}$

**Table 2**  
Boundary conditions.

	Measured value	CFD model parameter	Set value
Wall	30.1 °C	Constant wall temperature	30 °C
Ceiling	29.7 °C	Constant wall temperature	30 °C
Floor	29.8 °C	Constant wall temperature	30 °C
Lights	32.0 °C	Constant heat flux	36 w
Furniture	–	Constant heat flux	0 w

**Table 3**  
Setup of case parameters.

Case number	Inlet number	Air supply temperature t (°C)	Air supply velocity V (m/s)	Air supply direction D (°)	Distance between inlets d (m)
Case1	Inlet2	15	4	0	3.5
	Inlet5	27	4	0	
Case2	Inlet2	15	4	45	3.5
	Inlet5	27	4	45	
Case3	Inlet2	18	4	0	3.5
	Inlet5	24	4	0	
Case4	Inlet2	18	4	45	3.5
	Inlet5	24	4	45	
Case5	Inlet2	15	2	0	3.5
	Inlet5	27	2	0	
Case6	Inlet2	18	2	45	3.5
	Inlet5	24	2	45	
Group2 ( $\Delta t$ )	Inlets number	Air supply temperature t (°C)	Air supply velocity V (m/s)	Air supply direction D (°)	Distance between inlets d (m)
Case7	Inlet2	21	4	45	3.5
	Inlet5	21	4	45	
Δt = 0°C	Inlet2	19.5	4	45	
Δt = 3°C	Inlet5	22.5	4	45	3.5
Case4	Inlet2	18	4	45	
Δt = 6°C	Inlet5	24	4	45	3.5
Case9	Inlet2	16.5	4	45	
Δt = 9°C	Inlet5	25.5	4	45	3.5
Case2	Inlet2	15	4	45	
Δt = 12°C	Inlet5	27	4	45	3.5
Group3 (V)	Inlets number	Air supply temperature t (°C)	Air supply velocity V (m/s)	Air supply direction D (°)	Distance between inlets d (m)
Case10	Inlet2	21	4	45	3.5
	Inlet5	21	2	45	
Case7	Inlet2	21	4	45	3.5
	Inlet5	21	4	45	
Case11	Inlet2	21	4	45	3.5
	Inlet5	21	6	45	
Case12	Inlet2	21	4	45	3.5
	Inlet5	21	8	45	
Group4 ( location )	Inlets number	Air supply temperature t (°C)	Air supply velocity V (m/s)	Air supply direction D (°)	Distance between inlets d (m)
Case13	Inlet3	15	4	45	1.5
	Inlet4	27	4	45	
Case2	Inlet2	15	4	45	3.5
	Inlet5	27	4	45	
Case14	Inlet1	15	4	45	5.5
	Inlet6	27	4	45	
Case15	Inlet3	15	4	45 + 20(X)	1.5
	Inlet4	27	4	45-20(X)	
Case16 (Outlet2)	Inlet2	15	4	45	3.5
	Inlet5	27	4	45	

were based on reference data from the actual climate chamber. The heat source considered in the study was ceiling-mounted lights, which were also treated as Neumann boundary condition. The infrared ray thermometer (FLUKE 62 max+; A Fluke Company, USA) was used for wall surface temperature measurements, and the actual measured values are presented in Table 2. The surfaces of furniture were insulated. The air supply inlets were specified as velocity inlets, with a turbulence intensity set at 10% and a hydraulic diameter of 0.2 m. The air exhaust outlets were designated as outflows.

The RNG k- $\epsilon$  model [32] was chosen as turbulence model. The standard wall function was used to simulate the near-wall flow field [33] and the default discrete ordinates (DO) model was employed to calculate radiant heat transfer [34] and the emissivity of each wall was set to 0.9. To simulate buoyancy forces resulting from the variation of air density with temperature, indoor air was considered an ideal incompressible gas [35]. A second-order upwind scheme was applied to discretize the momentum, energy, and turbulence equations. The pressure-velocity coupling method used was the SIMPLE algorithm [36].

### 2.2.2. Case design

Four groups of cases were designed to investigate the effects of air supply direction (Group 1), air supply temperature (Group 2), air supply velocity (Group 3), and inlets location (Group 4) on ambient air temperature and velocity distribution, as well as the maximum level of thermal environmental differentiation achievable using this method. Details of the settings for each case are listed in Table 3. The upper limit of the air supply temperature was kept within the room temperature range to prevent energy waste from reheating.

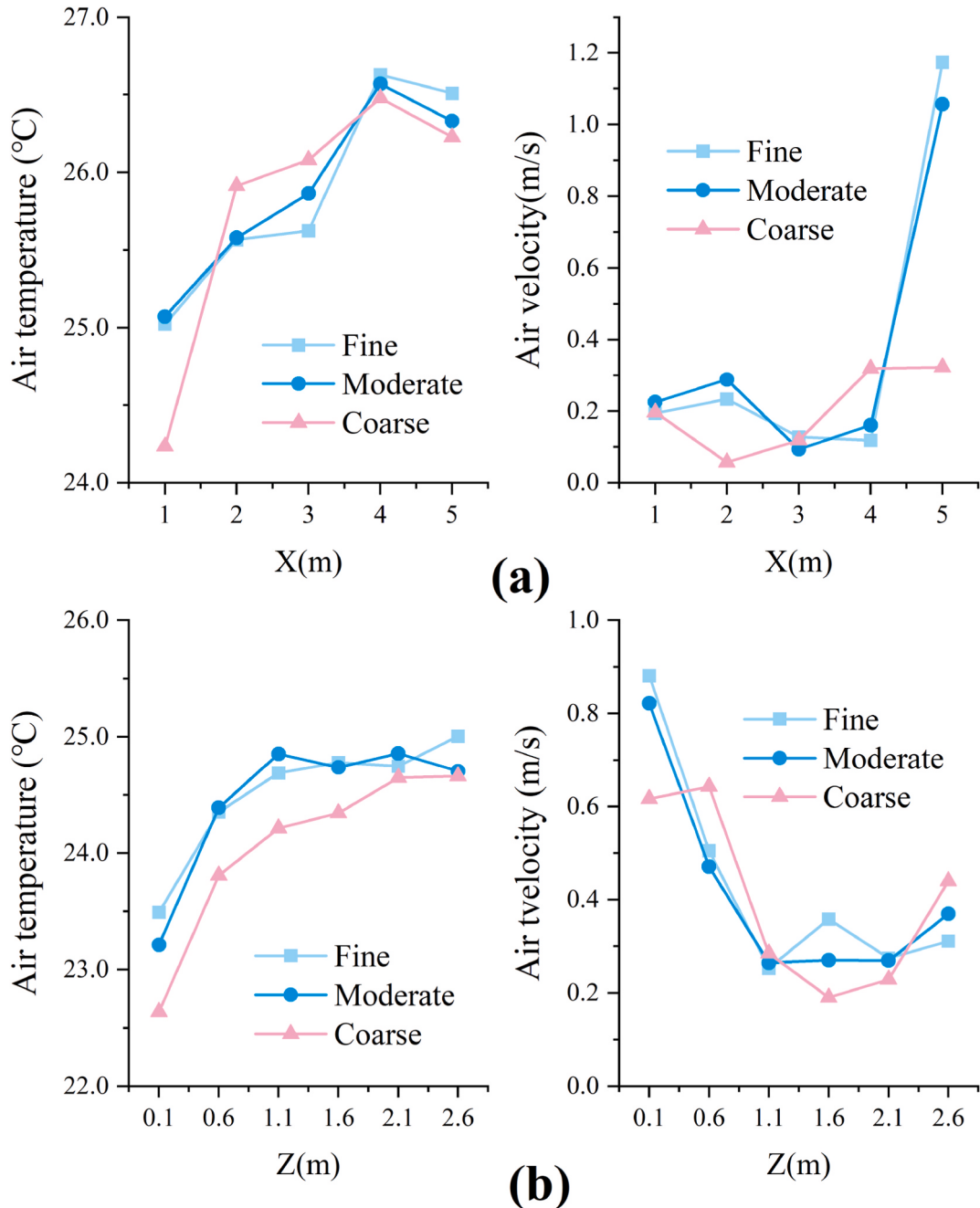


Fig. 2. Grid-independent test. (a) Line along the x-direction, at (y = 4.8 m, z = 0.6 m); (b) Line along the z-direction, at (x = 1.25 m, y = 4.8 m).

Meanwhile, the lower limit of the air supply temperature was set within the typical cooling range, which can go as low as 10 °C or even lower [37], aligning with the thermal comfort range of household air conditioners. The radiative temperatures in different zones were found to be generally consistent and are typically not directly controlled by convective air conditioning. Therefore, it was not discussed particularly.

(In order to investigate the effects of different factors, certain cases were repeated, and these repetitions are reflected in the Table 3 as well.)

### 2.2.3. Validation of the numerical model

To ensure the accuracy of the simulation results, grid-independent tests and comparisons between simulated and measured results were conducted. Three sets of grids, that was, 442,727(coarse), 814,587 (medium) and 1,613,667 (fine) grids, were generated. The comparison of air velocities and temperature distribution among the three grids is illustrated in Fig. 2. Temperature and velocity results were compared at line ( $y = 4.8 \text{ m}$ ,  $z = 0.6 \text{ m}$ ) along the x-direction and at line ( $x = 1.25 \text{ m}$ ,  $y = 4.8 \text{ m}$ ) along the z-direction. The boundary settings for Case 2 were used for grid-independent test. The results indicate that the air velocities and temperatures simulated with the moderate grid closely align with those obtained with the fine grid. In contrast, the air temperature calculated with the coarse grid exhibits significant deviation from the moderate and fine grids results. Consequently, the moderate grid was chosen, striking a balance between prediction accuracy and computational cost. The element quality registered at 0.83, displaying a negligible error of 0.007 and a minimum value of 0.37. The skewness values, peaking at 0.7 with a mean of 0.2 and a marginal error of 0.009.

In the validation case, inlet2, inlet5, outlet1 and outlet3 were used. The air supply parameters were set based on actual test values: Inlet2 had an air supply velocity of 3.34 m/s, a supply air temperature of 23.2 °C, and a supply air direction at a 45° angle with the horizontal; Inlet5 had an air supply velocity of 3.25 m/s, a supply air temperature of 22.9 °C, and a supply air direction at a 45° angle with the horizontal. The comparison between simulation and experimental results is presented in Fig. 3. Overall, the measured temperatures and velocities in the simulation were in good agreement with the experimental results, with an average absolute discrepancy of 0.2 °C for temperature and 0.14 m/s for velocity. However, there was a slight temperature discrepancy in the simulated results along Line-4. This discrepancy may be attributed to the fact that Line-4 is located near the table and between two supply air diffusers. In the simulation, the table was simplified as a solid rectangular block, neglecting the fact that there is empty space below the tabletop. Additionally, the supply air diffusers were simplified as rectangular inlets with uniform velocity distribution. These simplifications could lead to deviations between the simulated flow field and the actual conditions in this particular region. The maximum temperature discrepancy due to these simplifications was 1.3 °C (Line-8, at a height of 2.6 m), and the maximum velocity discrepancy

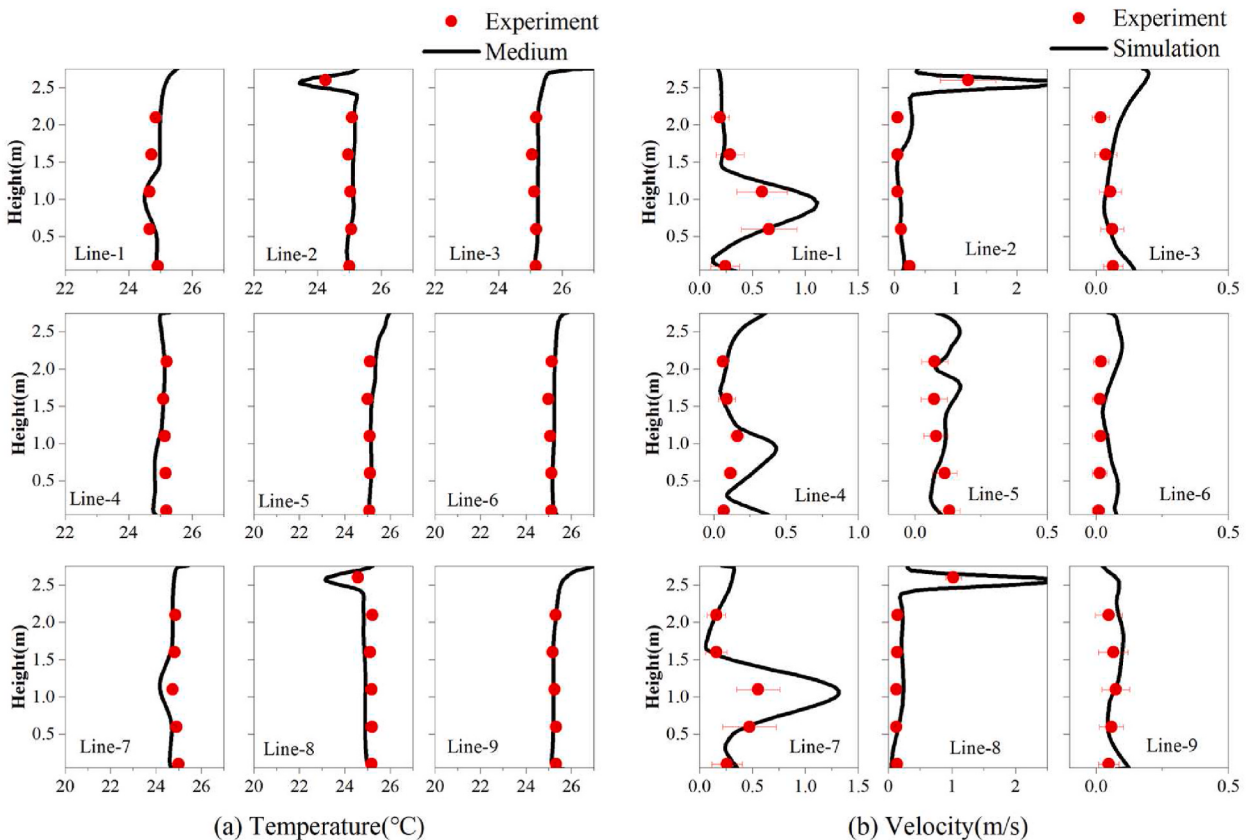


Fig. 3. Comparisons between simulated and measured results.

was 1.23 m/s (Line-2, at a height of 2.6 m). Nevertheless, overall, the simulation results were able to effectively capture the real-world scenario.

### 2.3. Evaluation method

#### 2.3.1. Evaluation indices

The analysis focused on the indoor air temperature and velocity for each case, as these are primarily affected by the air conditioner. In light of the combined impact of air temperature and velocity on human thermal sensation, the Cooling Effect was employed to convert air velocity into a numerical value expressed in the same unit as temperature.

In addition to thermal sensation, local discomfort is also crucial in air-conditioned rooms. Therefore, the draft rate (DR) at the head level (1.1 m) and the percentage of dissatisfied (PD) caused by the vertical temperature difference between 1.1 m and 0.1 m heights were calculated and analyzed. ASHRAE 55–2020 [38] was followed for the calculation of Cooling Effect and ISO 7730 [39] was employed for the assessment of local discomfort indices PD and DR, due to their formulaic clarity.

The calculation methods for each index are as follows:

- 1) **Cooling Effect (CE):** The calculation method follows the ASHRAE Standard 55–2020 [38]. equation (1) was used, where the original Standard Effective Temperature (SET) is calculated based on environmental and personal parameters, including airflow velocity ( $V_{elev}$ ), air temperature ( $T_a$ ), and radiant temperature ( $T_r$ ). The airflow velocity is then replaced by  $V_{still}$  (0.1 m/s), and the air temperature and radiant temperature are adjusted using the Cooling Effect (CE) to recalculate the SET, making the two SET values equal. Then, the Cooling Effect represents the equivalent cooling sensation caused by air velocities higher than 0.1 m/s under given conditions. A higher CE value indicates a cooler sensation provided by the air velocity in the environment.

$$SET(T_a, Tr, V_{elev}, *) = SET(Ta - CE, Tr - CE, V_{still}, *) \quad (1)$$

In the calculation, the clothing insulation was set at 0.57 clo, the metabolic rate was 1.0 met, and the relative humidity was 50% . The radiation temperature was based on the numerical simulation results.

- 2) **Equivalent Temperature (EqT):** In order to demonstrate more visually the reduction in thermal sensation caused by the Cooling Effect, the Equivalent Temperature (EqT) was introduced. EqT represents the equivalent perceived temperature based on human thermal sensation, considering the effects of air temperature and air velocity. Compared to SET, EqT provides a more concise and effective representation of the contribution of air temperature and air velocity to thermal environment differences, which was calculated by equation (2).

$$EqT = Air\ temperature\ (Ta) - Cooling\ effect\ (CE) \quad (2)$$

- 3) **Draught Rate (DR) and Percentage of Dissatisfied (PD) due to vertical temperature differences:** These two indices were applied to evaluate local discomfort, following the ISO 7730 [39]. DR was calculated based on the local air temperature, air velocity, and turbulence intensity at the head level (1.1 m) (the calculated parameters were all output from Fluent). PD was calculated based on the temperature difference between the head (1.1 m) and ankle (0.1 m) levels. Since the PD values for all cases were low, they were not illustrated separately but were included in the appendix. It was expected to maximize the differences in thermal environment at different locations while avoiding local discomfort.

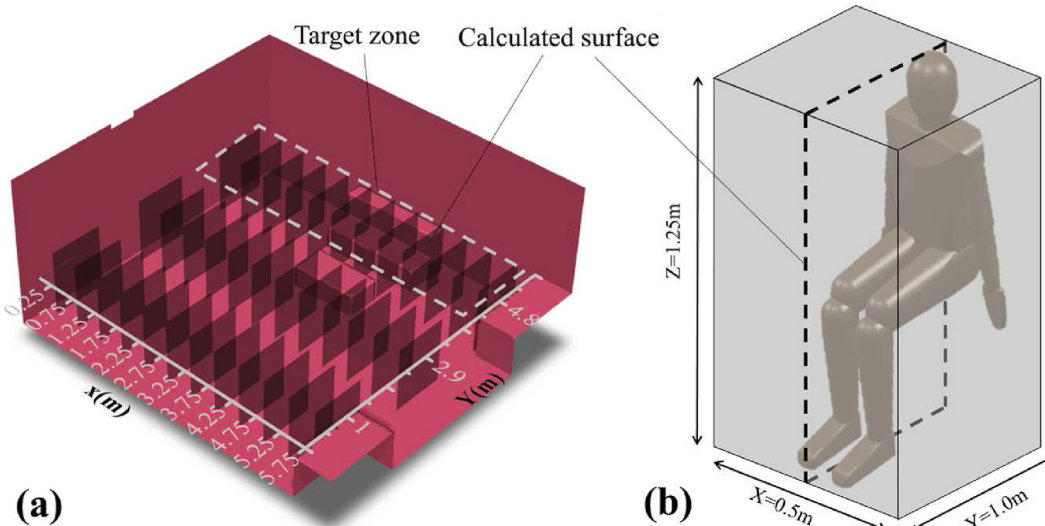


Fig. 4. Calculated surface.

### 2.3.2. Numerical data extraction method

Considering the human body dimensions in a seated posture, the human activity space was abstracted as a rectangular prism with a height of 1.25 m in the z-direction, a width of 0.5 m in the x-direction, and a length of 1.0 m in the y-direction. The vertical plane in the middle of x-direction was chosen as the calculated surface, and the average values on this plane were used to represent the overall parameters of the surrounding environment in the seated position. The values at the midpoint of 1.1 m and 0.1 m on the vertical plane are used for calculating DR and PD.

The positions of all calculated surfaces in the model are shown in Fig. 4 (a). Calculated surfaces were set every 0.5 m in the x-direction and at locations of 1.0 m, 2.9 m, and 4.8 m in the y-direction. The surfaces at Y = 4.8 m represented the main activity area of the occupants in spaces such as the living room, which was referred to as the "Target Zone" for subsequent analysis.

To analyze the differences in air temperature, air velocity, CE, EqT at different positions, the average values within each plane, especially the 12 surfaces in the Target Zone, were compared, including the air temperature differences, Equivalent Temperature differences, and gradients of average values along the x-direction for the 12 surfaces.

## 3. Result

### 3.1. Effect of air supply direction

In Case 1 and Case 2, the air was introduced through inlet 2 and inlet 5, while the exhaust air was extracted through outlet 1 and outlet 3. The supply air temperature difference was set to 12 °C, and the supply air velocity was 4 m/s for both cases. The difference lied in the direction of the supply air. In Case 1, the supply air was horizontally directed towards the positive y-axis, while in Case 2, it was directed towards the Target Zone at an angle of 45° with respect to the horizontal direction, as shown in Fig. 1, view (d).

In Fig. 5, the pink bars represent EqT (Ta - CE), and the blue portion represents the CE value. The value indicated at the top of the blue block corresponds to Ta. According to Fig. 5, both supply air directions could create significant air temperature differences ( $\Delta T_a$ ) at the row where Y = 4.8 m (Target Zone). The maximum  $\Delta T_a$  in different positions along the X-direction was 1.9 °C (Case 1) and 2.6 °C (Case 2). When considering the cooling effect caused by the air velocity, the maximum difference in EqT ( $\Delta EqT$ ) at different positions was 3.5 °C (Case 1) and 4.2 °C (Case 2). The distribution of CE differs between the two cases. With the 45° supply air direction, higher CE values were observed at X = 1 m and X = 5 m, which were opposite to the supply air vents, while the middle four positions had lower CE values. In the case of horizontal supply air, the position near X = 3 m showed higher CE values, which may be attributed to the downdraft encountering furniture at this location. Overall, within the Target Zone (Y = 4.8 m), the 45° supply air direction led to larger  $\Delta T_a$  and  $\Delta EqT$  at different positions along the X-direction compared to horizontal supply air. The average CE was smaller for horizontal supply air (1.7 °C) than for the 45° supply air (2.0 °C).

In areas outside the Target Zone, horizontal supply air resulted in larger  $\Delta T_a$  and  $\Delta EqT$ . At Y = 2.9 m, which was located below the air vents (at Y = 2.6 m), there was still a temperature difference in Case 1, reaching a maximum of 1.8 °C, close to the difference at Y =

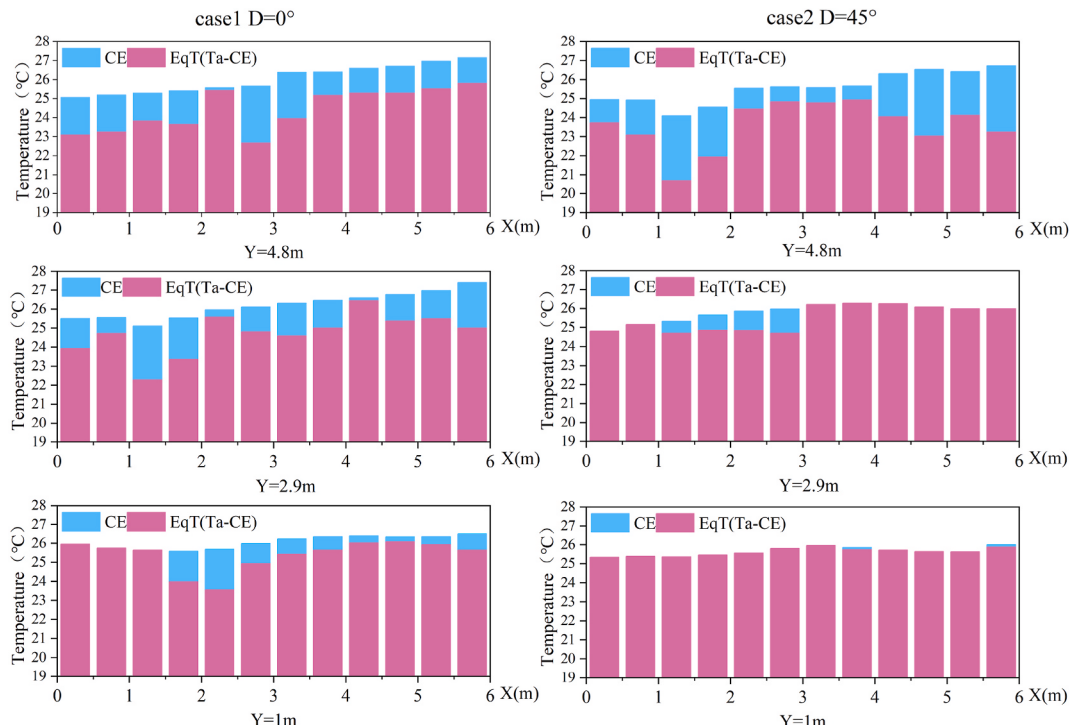


Fig. 5. Distribution of Temperature and CE under different supply air directions.

4.8 m. However, the temperature difference at  $Y = 2.9$  m in Case 2 decreased to  $1.5^\circ\text{C}$ . With  $45^\circ$  supply air, there was a cooling effect only at the left side near the lower temperature air supply vent, while the middle and right side temperatures were similar without Cooling Effect. At  $Y = 1$  m, on the opposite side of the supply air direction, the temperature difference in Case 2 almost disappeared, with a maximum temperature difference of only  $0.7^\circ\text{C}$ . The cooling effect is virtually negligible. The temperature difference caused by horizontal supply air was reduced to  $1.1^\circ\text{C}$ , indicating a small Cooling Effect still presented.

The simulation results for the other four conditions in Group 1, where the temperature difference was reduced to  $6^\circ\text{C}$  and the air velocity was reduced to 2 m/s, exhibit similar patterns to those observed in Case 1 and Case 2. Refer to the appendix for detailed results.

**Fig. 6** shows the air velocity distribution (a) at three Y positions for the six cases in Group1, as well as the Draught Rate (b) at the head height ( $Z = 1.1$  m) in the Target Zone.

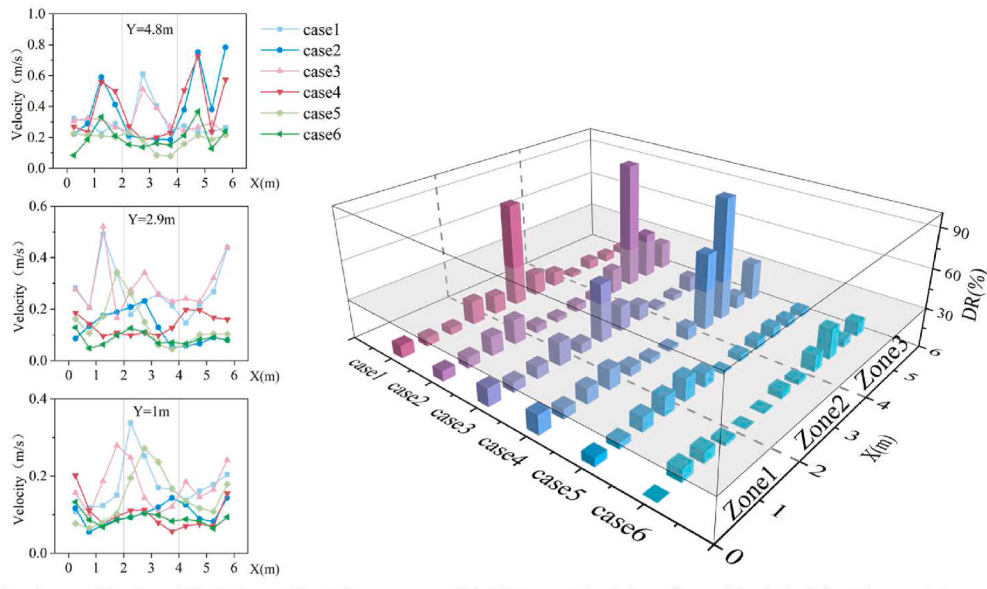
In the Target Zone, horizontal supply air (Case 1 and Case 3) resulted in higher velocity in the central area (between the two vertical dashed lines in the graph). On the other hand, the  $45^\circ$  supply air caused higher velocity in the left and right regions, aligning with the distribution of Cooling Effect. Similarly, the areas with Draught Rate exceeding 30% (ISO 7730 Category C) in graph (b) coincided with the regions of higher velocity. When the air supply velocity was reduced to 2 m/s for both supply vents, the velocity in these regions remained at a lower level, with the Draught Rate mostly below 30%. At  $Y = 2.9$  m and  $Y = 1$  m, compared to the Target Zone, all cases exhibited reduced velocity, with horizontal air supply resulting in relatively higher velocity.

**Fig. 7** provides a visual representation that helps to explain the simulated results mentioned above. Under horizontal supply air direction, lower temperatures and higher air velocities were observed in the lower region near the vents. On the other hand, under the  $45^\circ$  supply air direction, temperatures were relatively consistent between the area below the vents and the backside, and air velocities remained at lower levels.

### 3.2. Effect of air supply temperature difference

As explained in section 3.1 for Case 2, under  $45^\circ$  supply air direction, the Target Zone can be divided into three subzones based on the characteristics of air velocity and temperature. These subzones are defined as Zone 1, Zone 2, and Zone 3. Zone 1 consisted of the four leftmost positions with lower temperatures and higher air velocities. Zone 2 represents the middle four positions with moderate temperatures and the lowest air velocities. Zone 3 includes the four rightmost positions with higher temperatures and higher air velocities. In this section, the analysis focuses on these three regions and the differences in thermal environment across four calculated surfaces within each zone, under different air supply temperature differences.

The temperature difference between different zones increased with the increase in supply air temperature difference as shown in **Fig. 8**. When the supply air temperature difference reached  $6^\circ\text{C}$ , the differences between zones essentially reached their maximum values. Further increasing the temperature difference had a relatively small impact on the temperature disparities. When considering the Cooling Effect brought by air velocity, the EqT values in Zone 3 and Zone 1 were lower than those in Zone 2 for all cases. Zone 3 benefited from higher air velocities and thus experienced larger Cooling Effect, which could provide a lower thermal sensation even with higher temperatures. This characteristic could be utilized to achieve energy-efficient and comfortable operation in that zone. Except for the case with a  $0^\circ\text{C}$  supply air temperature difference, the maximum  $\Delta\text{EqT}$  values occurred between Zone 2 and Zone 3. The



(a) Velocity at  $Y = 1$  m,  $Y = 2.9$  m,  $Y = 4.8$  m      (b) DRs at  $Z = 1.1$  m (head height) in Target Zone

**Fig. 6.** The distribution of air velocity and Draught Rate (DR) under different air supply directions.

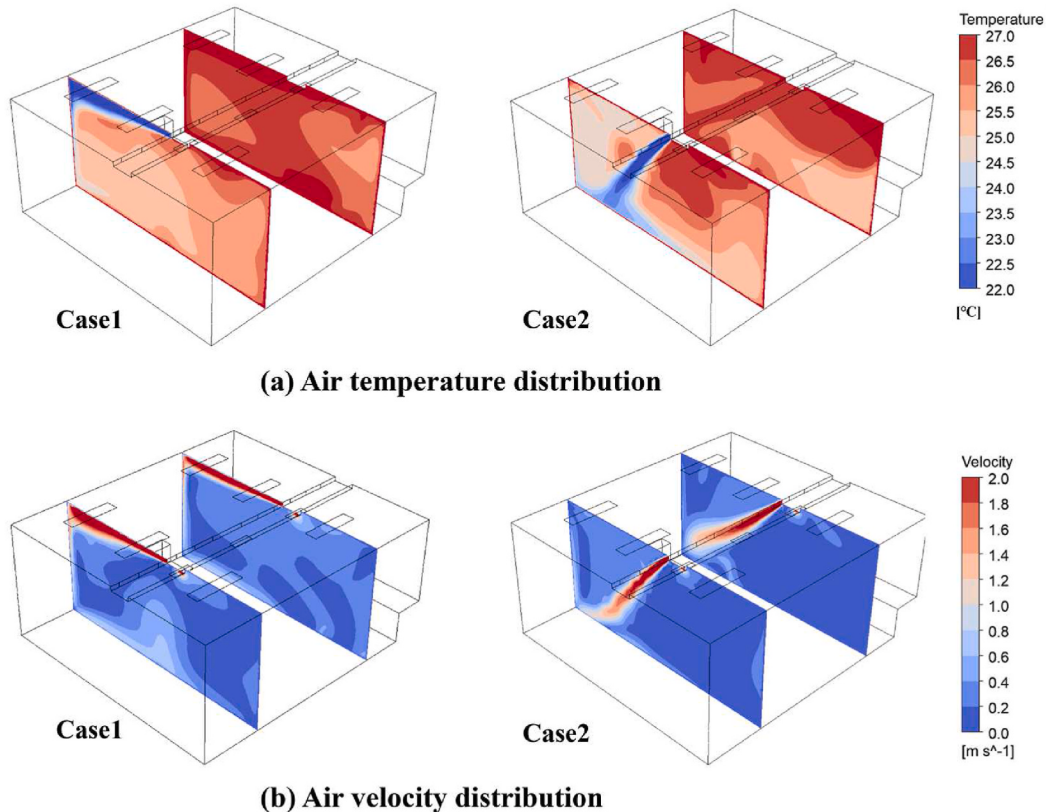


Fig. 7. Air temperature and velocity distributions under different air supply directions.

Cooling Effect in Zone 2 was influenced by various factors, including furniture layout and different airflow buoyancy caused by different supply air temperatures. The airflow structure in Zone 2 was more complex, resulting in complex variations in airflow velocity and temperature. Therefore, the Cooling Effect varied significantly under different supply air temperature differences.

In each zone, there were four calculated surfaces, and Fig. 9 shows more detailed temperature and velocity distributions with each calculated surface spaced 0.5 m apart. In (c) and (d) of Fig. 9, the temperature gradient results are represented by the gray shaded regions, which indicate the regression slope of temperature or Equivalent Temperature with respect to X, and the error bars represent the 95% confidence interval.

The temperature distribution pattern is evident, where the maximum temperature difference at different positions in the Target Zone and the temperature gradients within the shaded regions increased with the increase in supply air temperature difference. A supply air temperature difference of 6 °C proved sufficiently effective, generating an approximate temperature gradient of 0.6 °C/m. The lowest temperature was located at  $x = 0.75$  m, and the highest temperature was located at  $x = 5.75$  m, with a maximum

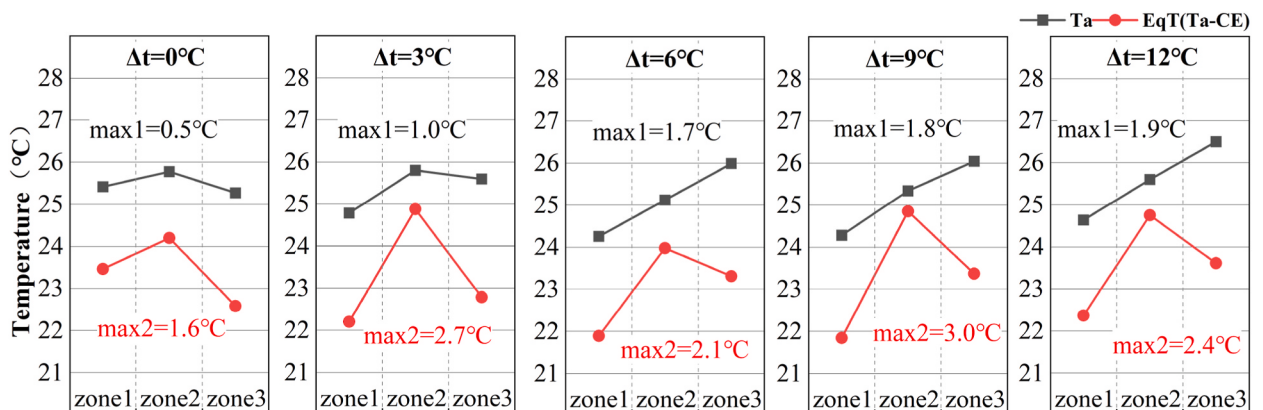
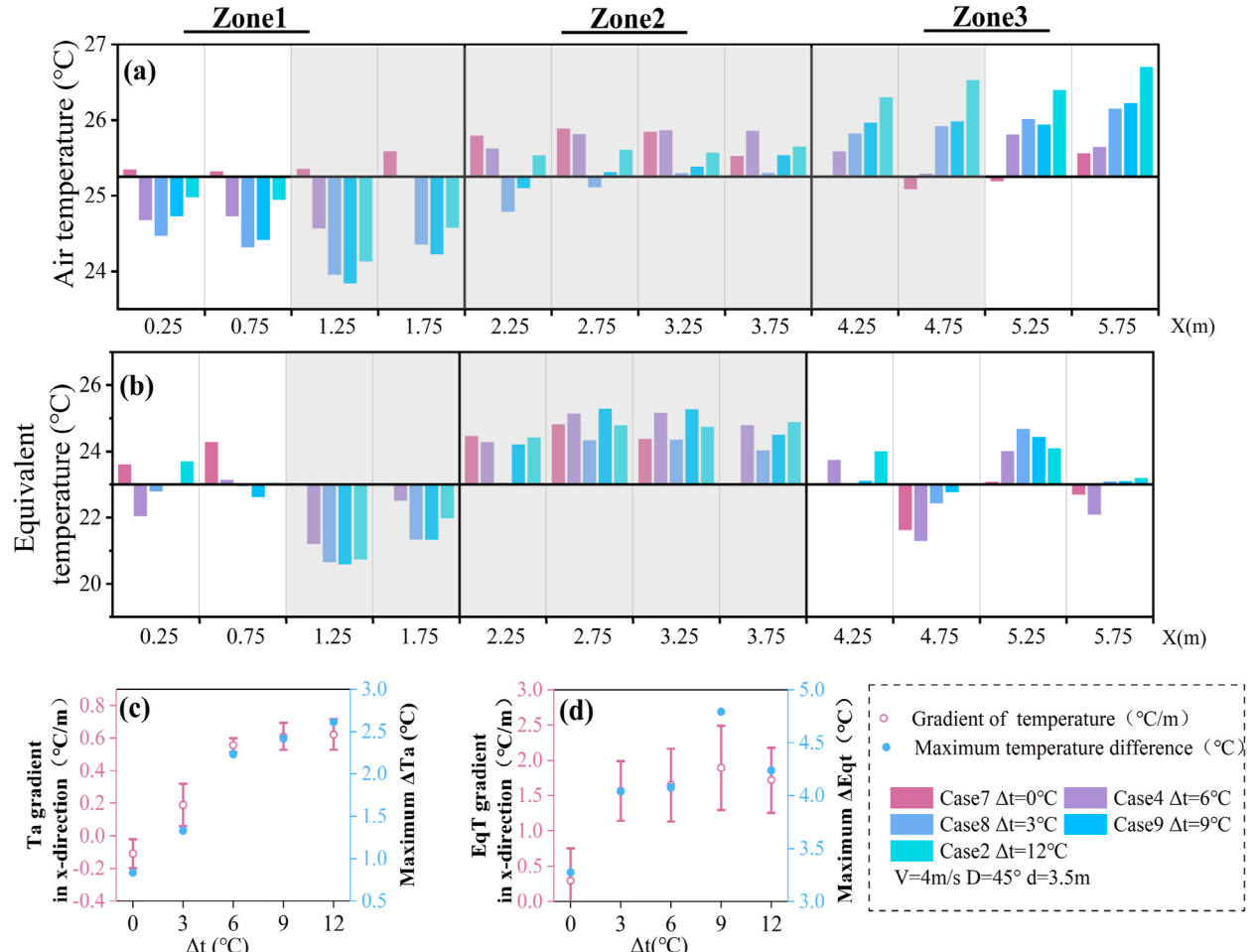


Fig. 8. The average temperature of subzones under different supply air temperature differences.



**Fig. 9.** Impact of air supply temperature differences on thermal environment, (a) Distribution of  $T_a$ , (b) Distribution of  $EqT$ , (c) Gradient and maximum difference of  $T_a$ , (d) Gradient and maximum difference of  $EqT$ .

temperature of  $2.6^{\circ}\text{C}$  (Case2).

When considering the Cooling Effect (CE) caused by air velocity, the Equivalent Temperature (EqT) gradient and the maximum  $\Delta EqT$  did not show a significant increase as the supply air temperature difference expanded. A supply air temperature difference of  $3^{\circ}\text{C}$  was already effective in creating significant EqT variations. When the supply air temperature difference exceeded  $3^{\circ}\text{C}$ , the maximum EqT difference essentially stabilized at around  $4.5^{\circ}\text{C}$ , with the exception of Case9, where lower airspeed in the central region led to a larger EqT difference. The EqT gradient also exhibited a similar trend, concentrating within the range of  $1.5\text{--}2.0^{\circ}\text{C}/\text{m}$ .

Fig. 10 illustrates the air velocity and Draught Rate (DR) values at different positions within the Target Zone. The air velocity distribution remained largely consistent across different supply air temperature differences. Zone 1 and Zone 3 exhibited higher air velocities, while Zone 2 had the lowest velocity. Zone 3 experienced the highest air velocity, which consequently resulted in a higher draught rate. Although Zone 1 was located in the cooler supply air region, the avoidance of direct airflow, similar to Zone 3, due to the influence of gravity on the cold air stream, resulted in relatively lower air velocity and DR. The distribution of air temperature for different cases is shown in Fig. 11, providing a visual representation that helps to explain the simulated results.

### 3.3. Effect of air supply velocity

When both air supply vents were set to deliver air at  $21^{\circ}\text{C}$ , with the left inlet (inlet2) at a fixed air supply velocity of  $4\text{ m/s}$  and the right inlet (inlet2) at air supply velocities of  $2\text{ m/s}$ ,  $4\text{ m/s}$ ,  $6\text{ m/s}$ , and  $8\text{ m/s}$ , the average temperature and average Equivalent Temperature (EqT) for the three zones are shown in Fig. 12. Firstly, the air temperature in Zone 1 and Zone 3 was slightly lower, and the air temperature difference among the three zones was within  $1^{\circ}\text{C}$ , so, the focus was primarily on the values of EqT. Increasing the air supply velocity at the right inlet had an impact on all three zones. When the air supply velocity at the right inlet reached  $8\text{ m/s}$ , the Cooling Effect (CE) in Zone 2 even expanded to around  $2^{\circ}\text{C}$ . This indicated that using air velocity to create thermal environment differences was feasible, but excessively large differences in air supply velocity might lead to unstable airflow patterns that were not conducive to creating differentiated thermal environments. This could result in synchronized increases in airflow velocity across

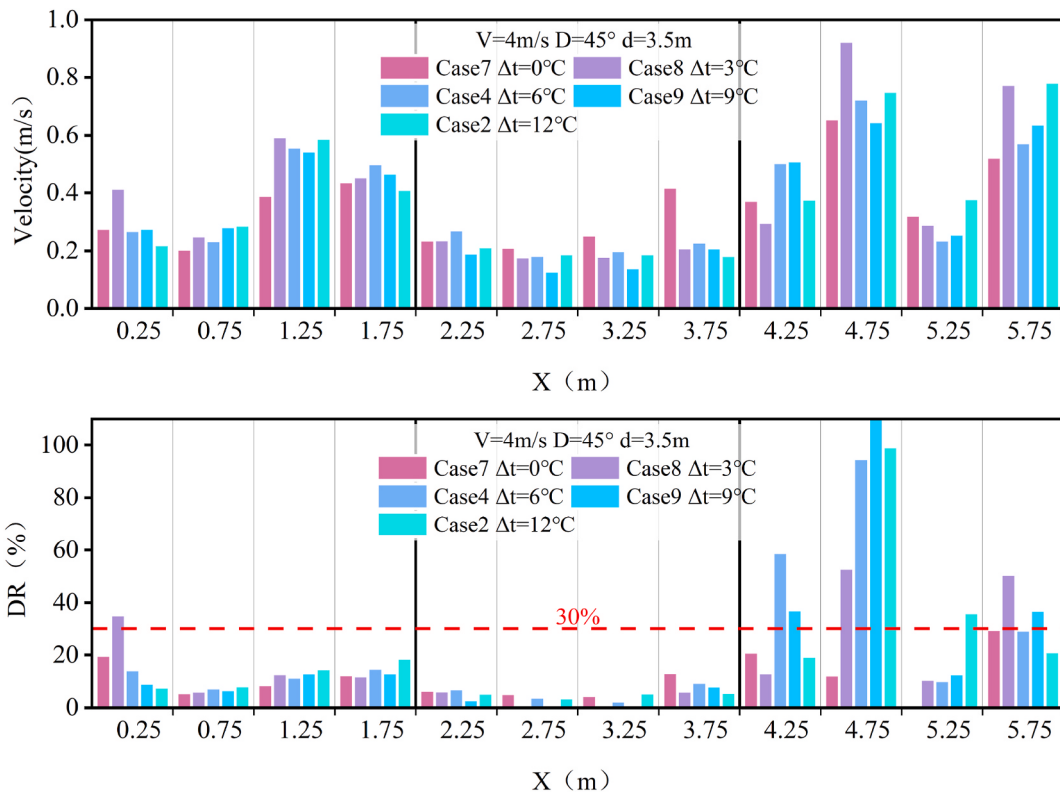


Fig. 10. Air velocity and Draught Rate (DR) distribution under different supply air temperature differences.

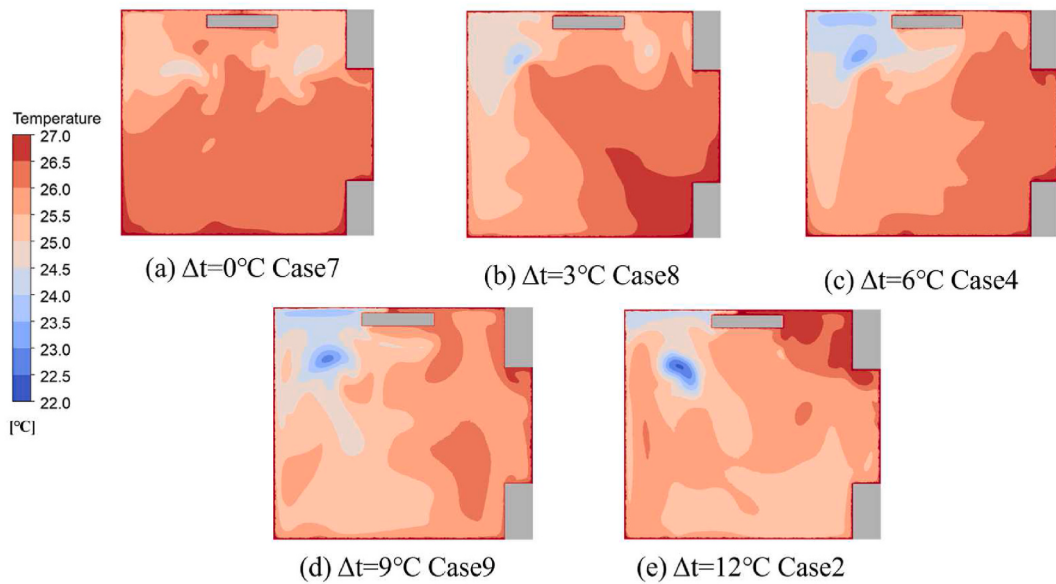


Fig. 11. Air temperature distribution at  $Z = 0.6$  m in different cases.

different zones, thereby reducing the level of differentiation. Conversely, lower air velocities resulted in smaller CE values that could not generate significant differences. The air supply velocity of 4 m/s & 6 m/s and 4 m/s & 8 m/s demonstrated similar effects on EqT differences among zones.

The specific temperature and air velocity distributions at each location are shown in Fig. 13. The temperature differences between different locations were around  $1^\circ\text{C}$ , and the level of differentiation in EqT followed the same pattern as the variations between zones.

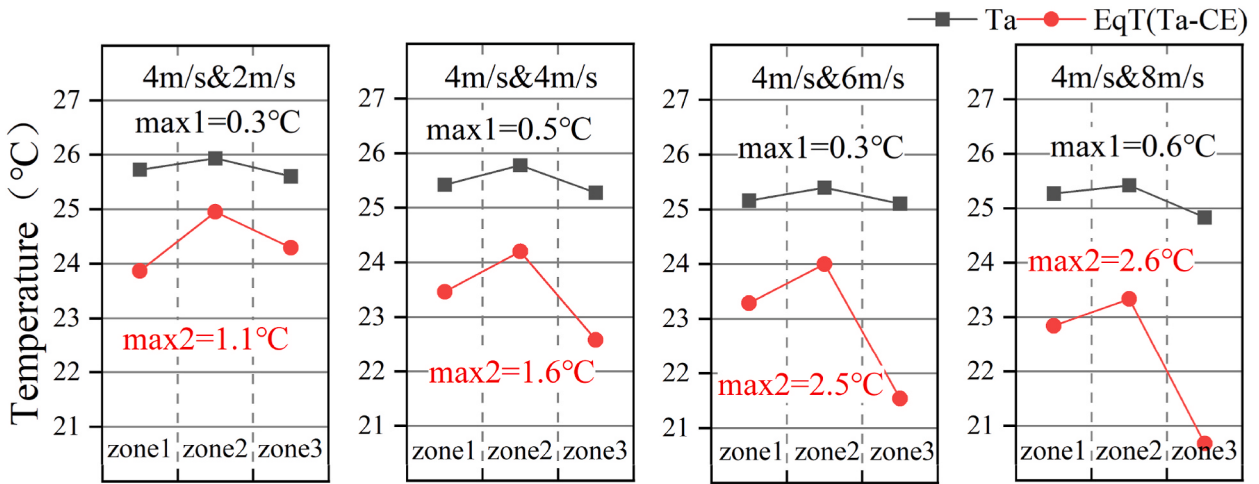


Fig. 12. The average temperature of subzones under different air supply velocity differences.

Specifically, when the air supply velocity at the right inlet reached 6 m/s, the EqT difference among different locations equaled that at 8 m/s. When the air supply velocity exceeded 4 m/s, zone 3 exhibited higher Draught Rate, indicating a stronger sensation of draft. It was advisable to avoid having individuals perceive thermal sensation at or below the neutral level in this zone. Among the four locations in Zone 2 where the sofa was located, the DR were generally below 30%. As this was the area where people were most likely to stay for extended periods, the EqT was relatively higher at the middle two positions ( $X = 2.75$  m and  $X = 3.25$  m) and lower at the two side positions ( $X = 2.25$  m and  $X = 3.75$  m).

### 3.4. Effect of vents location

Fig. 14 shows the influence of different distances between two air supply vents and the position of the exhaust air outlet on the air temperature, Equivalent Temperature (EqT), and air velocity at different locations. The difference between Case 2 and Case 15 was that Case 15 only had one return air outlet (outlet2) in the middle, while Case 2 had two return air outlets (outlet1 and outlet3) on both sides.

From Fig. 14(a) and (d), it can be observed that the temperature distribution in Case 15 and 2 was similar. This suggests that the impact of the number of return air outlets may be relatively minor. When the distance between the two supply air outlets was reduced, as shown in Fig. 14(b) (Case 13), maintaining the original air supply direction failed to separate the two airflows, resulting in reduced temperature difference between the left and right sides. By introducing an angle between the supply airflow direction and the vertical plane, i.e., directing the two supply air outlets towards the left and right sides respectively, the two airflows could be effectively separated, leading to a temperature gradient in the middle region (Fig. 14 (e)). When the distance between the two supply air outlets was increased, the position between the vents could still maintain a certain temperature gradient, but the temperature difference did not significantly increase. Therefore, it is important to avoid placing the air supply vents too close to each other. If it is unavoidable, adjusting the direction of the supply airflow can help separate the cool and warm airflows.

Fig. 15 shows a temperature contour map as the background, with blue arrows representing air velocity vectors. Due to buoyancy effects, the path of the cold airflow on the left side is lower than that of the hot airflow on the right side. Therefore, at the height of 0.6 m, the cold airflow primarily flowed from the left side to the right side. When the two supply air vents were too close together (Case 13), the high-speed regions of the two airflow streams mixed, but it also led to bifurcated airflows. By adjusting the supply air direction (Case 16), the mixing could be reduced and the expansion of the backflows towards the outer sides could be promoted, facilitating the formation of thermal environment differences. When the supply air vents were farthest apart (Case 14), the two airflow streams rotated inward, creating two distinct regions of backflow with noticeable temperature differences.

## 4. Discussion

### 4.1. The significance of the Equivalent Temperature index

The concept of Equivalent Temperature used in this study represents the air temperature (Ta) minus the Cooling Effect (CE), providing an objective assessment of the combined impact of air temperature and air velocity on human thermal sensation.

The widely adopted Predicted Mean Vote (PMV) serves as a significant metric in the field of thermal comfort, offering a direct prediction of human thermal sensation based on calculating environmental and individual parameters. Fig. 16 depicts the PMV values at various locations, computed according to the ASHRAE Standard 55–2020 [38], using the same parameters as those utilized for determining the Cooling Effect, as described in Section 2.3.1. In general, the PMV values aligned with the corresponding levels observed for the Equivalent Temperature (EqT) metric in the study. Lower PMV values in zones 1 and 3 indicated a bias towards colder thermal sensation, while the intermediate Zone 2 exhibited relatively higher PMV values.

By utilizing both Ta and CE as individual metrics and the Equivalent Temperature derived from their combination, this research

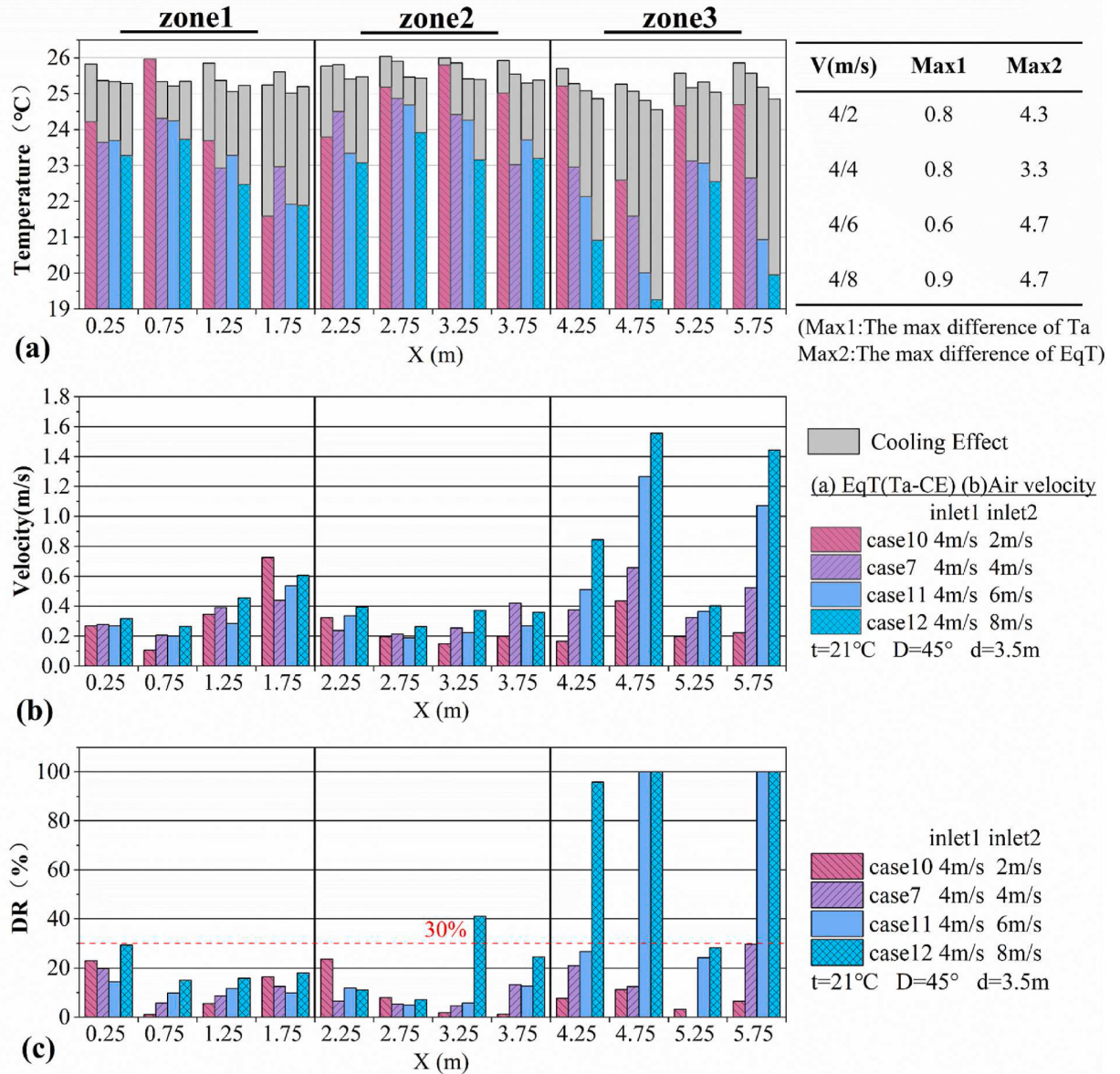


Fig. 13. Distribution of  $\text{Ta}$ ,  $\text{EqT}$ ,  $\text{Va}$ , and  $\text{DR}$  under different air supply velocity differences.

provides a more direct reflection of the thermal sensation difference resulting from air temperature and air velocity.

#### 4.2. Practical application

Typically, individual differences in comfort temperature due to factors such as gender, age, and BMI are generally within a range of  $1^{\circ}\text{C}$  or even smaller [10,14]. Apart from individual variations, differences in metabolic rates among people, which arise from variations in activity levels, contribute to varying thermal demands. In this section, differences in metabolic rates are used to represent variations in states among individuals, illustrating the potential of the dual air supply system in meeting diverse thermal requirements, as shown in Fig. 17. Different points are positioned based on the operating temperature and velocity of two Cases. Distinct color regions represent the comfort intervals corresponding to the respective metabolic rates, calculated based on PMV within  $\pm 0.5$ . The results suggest that by adjusting the supply air temperature (Case 9) and supply air velocity (Case 11), the system can reasonably accommodate the requirements of four different metabolic rates. Moreover, the variation in air velocity is identified as a crucial factor in achieving this outcome.

The potential practical implementation scenarios are illustrated in Fig. 18. In practical applications, it is recommended to fully utilize the differences in thermal sensation caused by air temperature and air velocity. However, considerations should also be given to

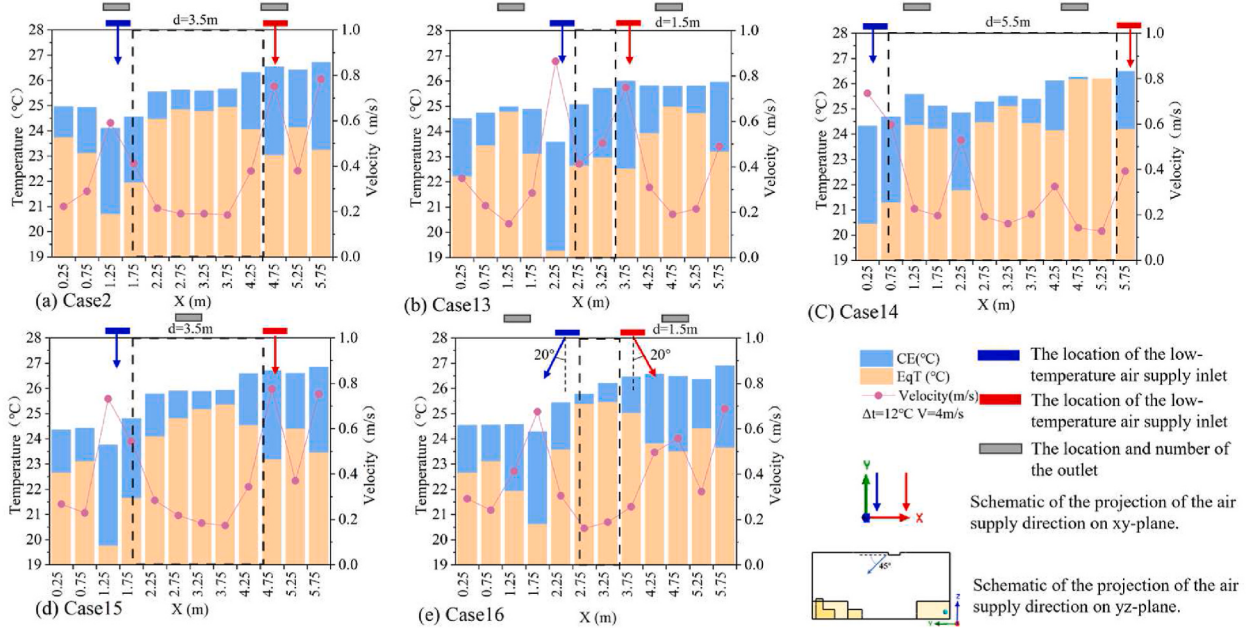


Fig. 14. Temperature distribution under different air supply vent positions.

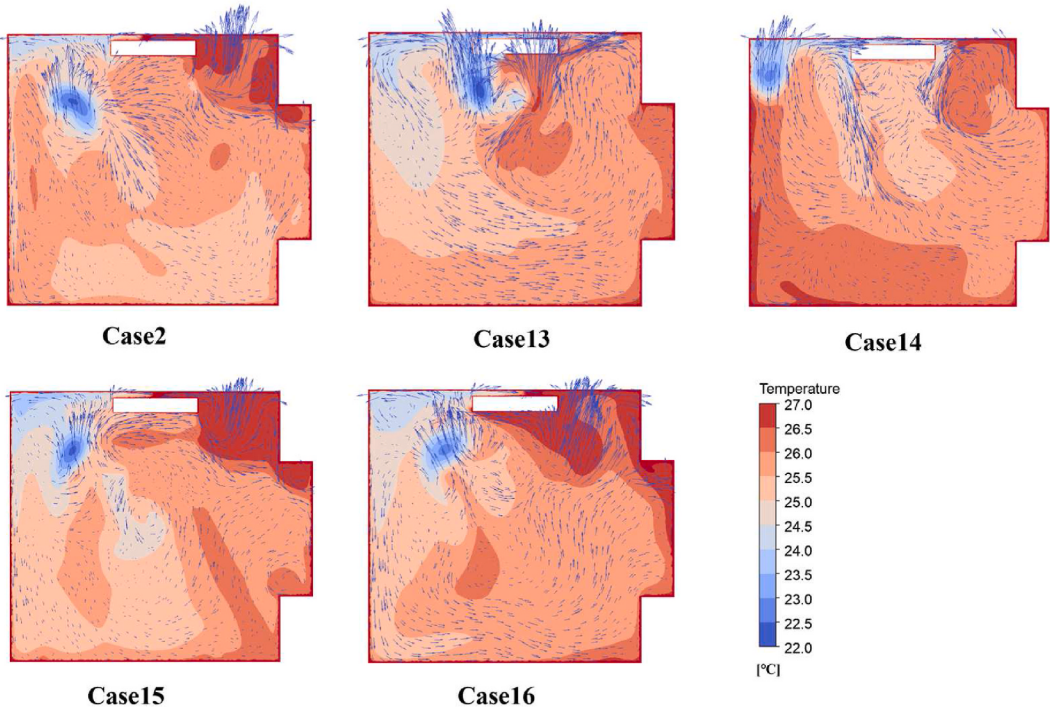


Fig. 15. Temperature distribution and air velocity vector map at  $z = 0.6$  m height.

individuals' lifestyle preferences. When two individuals are seated on the sofa in Zone 2 (middle area in Target Zone), the lower air velocity in that area may result in minimal localized discomfort, and the temperature differences across different positions range from 0 to 1.1 °C (Case9), which generally satisfy individual variations during sedentary activities. However, for individuals with higher thermal comfort preferences due to physical activities or other factors, it is advisable to seek locations in Zone 1 (left area in Target Zone) or Zone 3 (right area in Target Zone) where higher air velocities can be utilized.

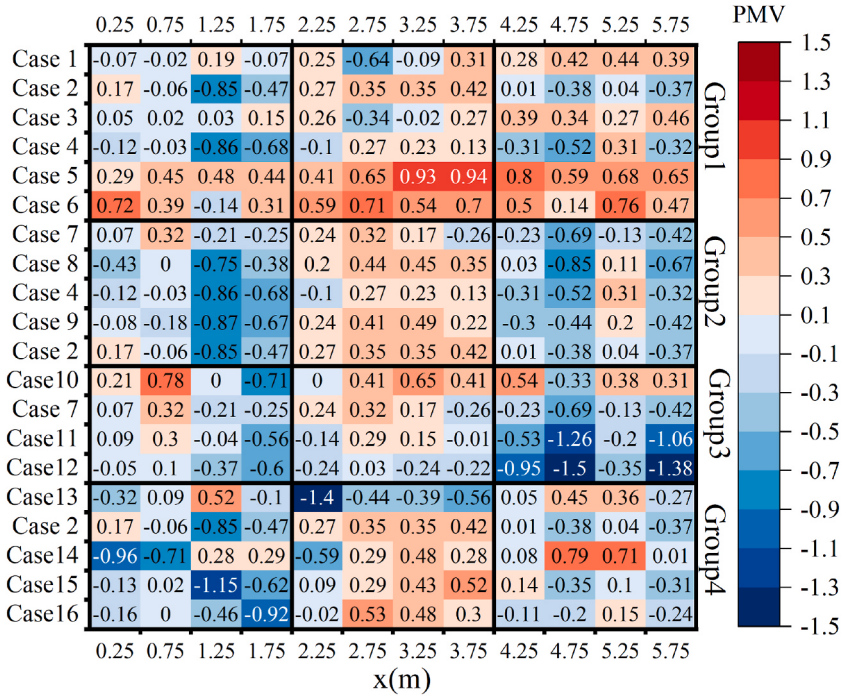


Fig. 16. PMV values at different locations in different cases.

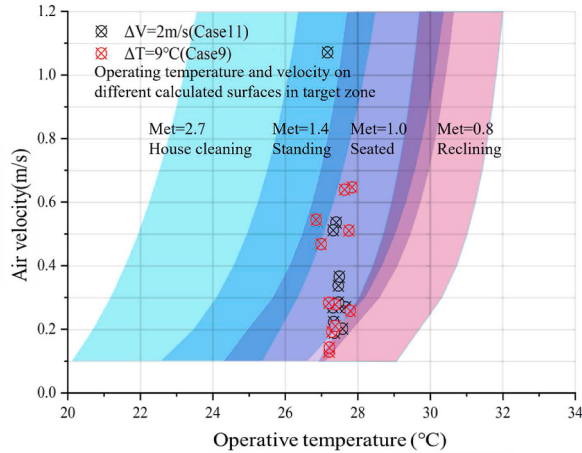


Fig. 17. The potential of dual air supply conditioning to meet diverse thermal requirements.

#### 4.3. Effect of occupants

To assess the thermal disturbance caused by occupants, the environmental conditions of Case 2 were employed, and manikins were introduced (see Fig. 19). Two manikins were positioned at  $x = 1.25$  m and  $x = 4.75$  m in target zone, simulating seated postures (68W each). Despite the introduction of manikins, the temperature variations across different planes were minimal, averaging  $0.2^{\circ}\text{C}$ . PMV values were used for a comprehensive evaluation of the manikins' impact on the temperature, air velocity, and radiation fields. The average PMV variation across all planes was 0.2. Overall, using the model without manikins still provided a reasonably accurate prediction of scenarios involving human activities.

#### 4.4. Limitation

Since refrigeration is the main focus of residential air conditioning systems during the summer, this study primarily simulated the conditions during the cooling season. The patterns and thermal comfort levels under heating conditions have not been investigated in this study.

In numerical simulations of indoor environments, it is common to incorporate human body models to explore the impact of human

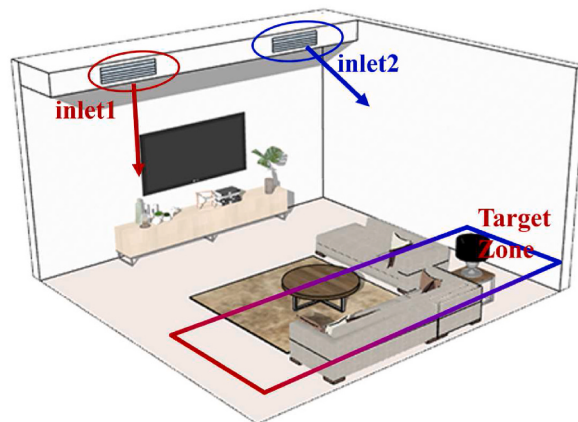


Fig. 18. Examples of practical application scenarios.

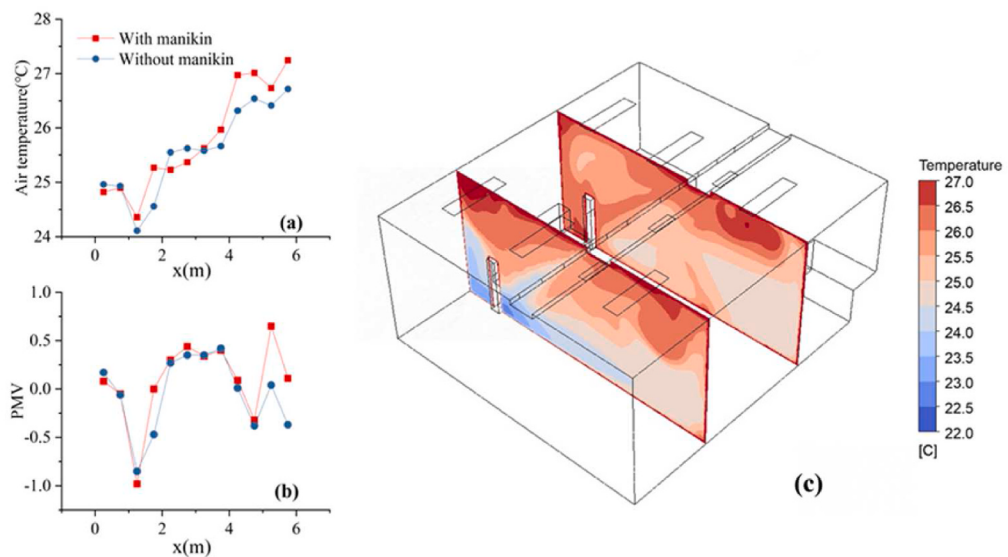


Fig. 19. The impact of occupants on simulation results.

heat dissipation on the environment. However, this type of simulation is feasible for environments such as classrooms and offices where individuals generally occupy fixed positions. In residential environments, individuals have a larger range of activities, and fixing the human body model in one position lacks representativeness and significance. Therefore, in the numerical simulations conducted in this study, the consideration of human heat dissipation has not been included.

## 5. Conclusion

The potential of creating differentiated thermal environments using two air supply vents on a single air conditioner was investigated. The effects of air supply direction, air supply temperature, air supply velocity, and vent location on the distribution of air temperature and air velocity were analyzed. The differentiation level of the thermal environment was evaluated by assessing the air temperature and the Equivalent Temperature that incorporates the Cooling Effect at different locations within the Target Zone of air conditioning. The main conclusions are as follows:

- 1) In the Target Zone of air conditioner, three distinct zones could be created: a high-temperature/high-velocity zone, a low-temperature/high-velocity zone, and a medium-temperature/low-velocity zone. Among them, the high-temperature/high-velocity zone provided comfortable and energy-efficient operation, while the medium-temperature/low-velocity zone was the warmest and the low-temperature/high-velocity zone was the coolest. Furthermore, the draught rate in the medium-temperature/low-velocity zone was minimized. Taking into account the Cooling Effect, the maximum Equivalent Temperature difference among the three zones could reach around 3.0 °C. The research results demonstrated the feasibility of using dual air supply vents on the air conditioner to create diversified thermal environments.

- 2) By controlling the air supply temperature difference, the Equivalent Temperature difference among different calculated surfaces within the Target Zone could reach around 4.5 °C, which was possible to meet the common individual thermal demand differences. A supply air temperature difference of 6 °C was already effective in creating a differentiated thermal environment.
- 3) Fully utilizing the disparities in air velocity was found to be an effective approach in achieving distinct thermal environments. In the experimental conditions, when two vents supplied air at velocities of 4 m/s and 6 m/s respectively, the maximum Equivalent Temperature difference could be observed within the Target Zone.
- 4) Compared to horizontally oriented supply airflow, directing airflow towards the Target Zone resulted in greater temperature differences and Equivalent Temperature differences at various positions within the zone. When the two supply vents were positioned too closely, it was necessary to adjust the airflow direction to separate the airflows, ensuring temperature differences and Equivalent Temperature differences at different positions.

#### CRediT authorship contribution statement

**Yuxin Yang:** Writing – original draft, Investigation, Formal analysis, Data curation, Validation. **Zisheng Zhao:** Writing – original draft, Conceptualization. **Junmeng Lyu:** Writing – review & editing. **Bo Wang:** Writing – review & editing. **Jinbo Li:** Writing – review & editing. **Shuguang Zhang:** Writing – review & editing. **Zhiwei Lian:** Conceptualization, Writing – review & editing, Methodology, Funding acquisition, Conceptualization.

#### Declaration of competing interest

The authors declare that they have no known competing financial interests or personal relationships that could have appeared to influence the work reported in this paper.

#### Data availability

Data will be made available on request.

#### Acknowledgements

This work is supported by the National Key R&D Program of China (2022YFC3803201).

#### Appendix

The PD values were calculated for all cases at various positions within the Target Zone, with a maximum value not exceeding 3%. Therefore, it is unlikely that this method would cause local discomfort resulting from vertical temperature differences.

**Table I**  
The dissatisfaction rate (PD) caused by vertical temperature difference

x	0.25	0.75	1.25	1.75	2.25	2.75	3.25	3.75	4.25	4.75	5.25	5.75
Case1	0.51	0.48	0.33	0.29	0.12	0.14	0.39	0.25	0.12	0.16	0.19	0.20
Case2	0.50	0.82	1.27	1.10	2.12	1.45	1.12	1.47	0.29	0.31	0.23	0.28
Case3	0.33	0.33	0.24	0.33	0.10	0.08	0.20	0.25	0.26	0.31	0.29	0.30
Case4	0.37	0.42	0.50	0.36	0.30	0.29	0.47	0.32	0.27	0.29	0.31	0.26
Case5	0.67	1.02	0.72	0.79	0.17	0.28	0.13	0.14	0.23	0.33	0.32	0.19
Case6	0.50	0.57	1.71	3.03	1.70	1.25	0.71	0.99	0.80	0.69	0.42	0.27
Case7	0.37	0.38	0.43	0.67	0.68	0.63	0.47	0.45	0.48	0.57	0.41	0.26
Case8	0.32	0.41	0.66	0.37	0.32	0.32	0.29	0.22	0.40	0.43	0.40	0.27
Case9	0.66	0.69	0.78	0.85	1.04	0.92	0.80	0.89	0.26	0.25	0.24	0.25
Case10	0.29	0.40	0.85	0.95	0.58	0.56	0.35	0.33	0.47	0.50	0.44	0.37
Case11	0.41	0.45	0.52	0.97	0.84	0.68	0.47	0.42	0.39	0.21	0.34	0.28
Case12	0.30	0.70	0.62	0.99	0.58	0.41	0.26	0.26	0.39	0.24	0.35	0.29
Case13	0.26	0.59	0.88	1.41	1.22	2.80	2.28	0.29	0.36	0.43	0.37	0.27
Case14	0.23	0.24	0.80	0.43	0.10	0.15	0.26	0.20	0.37	0.17	0.20	0.27
Case15	0.44	0.72	1.43	1.26	1.24	0.72	0.54	0.57	0.26	0.25	0.20	0.27
Case16	0.36	0.47	1.63	1.55	1.18	0.72	1.11	0.98	0.25	0.20	0.21	0.25

In response to the simulation results mentioned in the main text, the detailed findings for the other four conditions in Group 1, where the temperature difference was reduced to 6 °C and the air velocity was reduced to 2 m/s, have been presented in Fig.I The observed patterns in these conditions were similar to those observed in Case 1 and Case 2, further supporting the conclusions drawn from the main analysis.

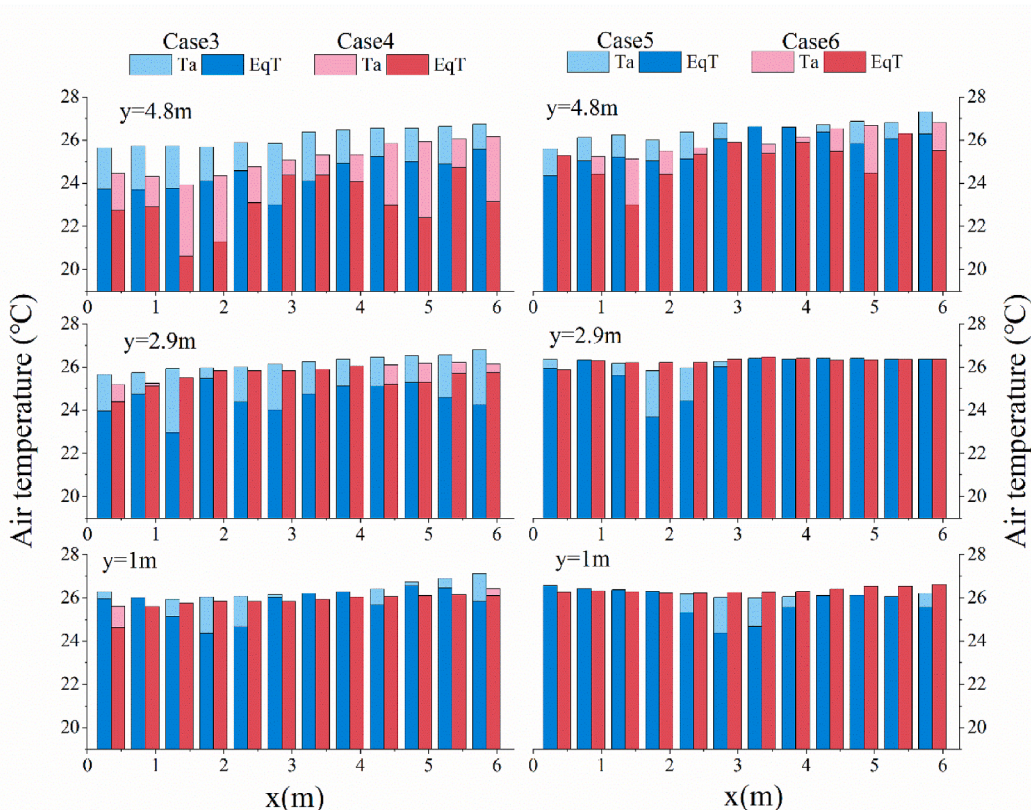


Fig. I. Air temperature and EqT calculation results for Case 3 to Case 6.

## References

- [1] H. Yan, F. Shi, Z. Sun, G. Yuan, M. Wang, M. Dong, Thermal adaptation of different t point temperature modes and energy saving potential in split air-conditioned office buildings during summer, *Build. Environ.* 225 (Nov. 2022), 109565, <https://doi.org/10.1016/j.buildenv.2022.109565>.
- [2] J. Lyu, et al., How do people set air conditioning temperature setpoint in urban domestic-Behavior model in Chinese three climate zones based on historical usage data, *Energy Build.* 284 (Apr. 2023), 112856, <https://doi.org/10.1016/j.enbuild.2023.112856>.
- [3] Z. Wang, et al., Individual difference in thermal comfort: a literature review, *Build. Environ.* 138 (Jun. 2018) 181–193, <https://doi.org/10.1016/j.buildenv.2018.04.040>.
- [4] P.O. Fanger, *Thermal comfort. Analysis and Applications in Environmental Engineering*, Danish Technical Press, Copenhagen, 1970.
- [5] H. Du, et al., Gender differences in thermal comfort under coupled environmental factors, *Energy Build.* 295 (2023), 113345, <https://doi.org/10.1016/j.enbuild.2023.113345>.
- [6] J. Lyu, H. Du, Z. Zhao, Y. Shi, B. Wang, Z. Lian, Where should the thermal image sensor of a smart A/C look?-Occupant thermal sensation model based on thermal imaging data, *Build. Environ.* 239 (2023), 110405, <https://doi.org/10.1016/j.buildenv.2023.110405>.
- [7] J. van Hoof, L. Schellen, V. Soebarto, J.K.W. Wong, J.K. Kazak, Ten questions concerning thermal comfort and ageing, *Build. Environ.* 120 (Aug. 2017) 123–133, <https://doi.org/10.1016/j.buildenv.2017.05.008>.
- [8] Y. Wu, et al., Age differences in thermal comfort and physiological responses in thermal environments with temperature ramp, *Build. Environ.* 228 (Jan. 2023), 109887, <https://doi.org/10.1016/j.buildenv.2022.109887>.
- [9] J. Xiong, T. Ma, Z. Lian, R. de Dear, Perceptual and physiological responses of elderly subjects to moderate temperatures, *Build. Environ.* 156 (Jun. 2019) 117–122, <https://doi.org/10.1016/j.enbuild.2019.04.012>.
- [10] M. Indraganti, R. Ooka, H.B. Rijal, Thermal comfort in offices in India: behavioral adaptation and the effect of age and gender, *Energy Build.* 103 (2015) 284–295, <https://doi.org/10.1016/j.enbuild.2015.05.042>.
- [11] M. Fountain, G. Brager, R. de Dear, Expectations of indoor climate control, *Energy Build.* 24 (3) (1996) 179–182, [https://doi.org/10.1016/S0378-7788\(96\)00988-7](https://doi.org/10.1016/S0378-7788(96)00988-7).
- [12] A.M.J. van Ooijen, W.D. van Marken Lichtenbelt, K.R. Westerterp, Individual differences in body temperature and the relation to energy expenditure: the influence of mild cold, *J. Therm. Biol.* 26 (4) (Sep. 2001) 455–459, [https://doi.org/10.1016/S0306-4565\(01\)00060-2](https://doi.org/10.1016/S0306-4565(01)00060-2).
- [13] S. Karjalainen, Thermal comfort and gender: a literature review, *Indoor Air* 22 (2) (2012) 96–109, <https://doi.org/10.1111/j.1600-0668.2011.00747.x>.
- [14] L. Lan, Z. Lian, W. Liu, Y. Liu, Investigation of gender difference in thermal comfort for Chinese people, *Eur. J. Appl. Physiol.* 102 (4) (2008) 471–480, <https://doi.org/10.1007/s00421-007-0609-2>.
- [15] Y. Wu, J. Fan, B. Cao, Comparison among different modeling approaches for personalized thermal comfort prediction when using personal comfort systems, *Energy Build.* 285 (2023), 112873, <https://doi.org/10.1016/j.enbuild.2023.112873>.
- [16] W. Pasut, H. Zhang, E. Arens, Y. Zhai, Energy-efficient comfort with a heated/cooled chair: results from human subject tests, *Build. Environ.* 84 (Jan. 2015) 10–21, <https://doi.org/10.1016/j.buildenv.2014.10.026>.
- [17] B. Liu, H. Wang, K. Ji, B. Ge, X. Zhang, Using personal comfort systems during the post-heating season in a cold climate: a field study in offices, *Case Stud. Therm. Eng.* 45 (May 2023), 102974, <https://doi.org/10.1016/j.csite.2023.102974>.

- [18] R. Rissetto, M. Schweiker, A. Wagner, Personalized ceiling fans: effects of air motion, air direction and personal control on thermal comfort, Energy Build. 235 (2021), 110721, <https://doi.org/10.1016/j.enbuild.2021.110721>.
- [19] D. He, N. Li, Y. He, M. He, C. Song, H. Chen, Experimental study on thermal sensation of radiant cooling workstation and desktop fan in hot-humid environment, Procedia Eng. 205 (2017) 757–764, <https://doi.org/10.1016/j.proeng.2017.10.007>.
- [20] S. Watanabe, T. Shimomura, H. Miyazaki, Thermal evaluation of a chair with fans as an individually controlled system, Build. Environ. 44 (7) (Jul. 2009) 1392–1398, <https://doi.org/10.1016/j.buildenv.2008.05.016>.
- [21] A.K. Melikov, Personalized ventilation, Indoor Air 14 (Suppl 7) (Jan. 2004) 157–167, <https://doi.org/10.1111/j.1600-0668.2004.00284.x>.
- [22] J. Lyu, Y. Shi, H. Du, Z. Lian, Sex-based thermal comfort zones and energy savings in spaces with joint operation of air conditioner and fan, Build. Environ. (Oct. 2023), 111002, <https://doi.org/10.1016/j.buildenv.2023.111002>.
- [23] H. Zhang, E. Arens, Y. Zhai, A review of the corrective power of personal comfort systems in non-neutral ambient environments, Build. Environ. 91 (Sep. 2015) 15–41, <https://doi.org/10.1016/j.buildenv.2015.03.013>.
- [24] Y. Liu, Y. Liu, X. Shao, Y. Liu, C.-E. Huang, Y. Jian, Demand-oriented differentiated multi-zone thermal environment: regulating air supply direction and velocity under stratum ventilation, Build. Environ. 219 (Jul. 2022), 109242, <https://doi.org/10.1016/j.buildenv.2022.109242>.
- [25] X. Shao, K. Wang, X. Li, Z. Lin, Potential of stratum ventilation to satisfy differentiated comfort requirements in multi-occupied zones, Build. Environ. 143 (Oct. 2018) 329–338, <https://doi.org/10.1016/j.buildenv.2018.07.029>.
- [26] Y. Zhao, W. Li, C. Jiang, Thermal sensation and occupancy-based cooperative control method for multi-zone VAV air-conditioning systems, J. Build. Eng. 66 (May 2023), 105859, <https://doi.org/10.1016/j.jobe.2023.105859>.
- [27] X. Shan, N. Luo, K. Sun, T. Hong, Y.-K. Lee, W.-Z. Lu, Coupling CFD and building energy modelling to optimize the operation of a large open office space for occupant comfort, Sustain. Cities Soc. 60 (Sep. 2020), 102257, <https://doi.org/10.1016/j.scs.2020.102257>.
- [28] J. Hu, C. Shan, J. Wu, A. Zhang, G. Ding, L.X. Xu, A cooperative ceiling air supply method to satisfy personal thermal preferences in a discretionary indoor position, J. Build. Eng. 31 (Sep. 2020), 101367, <https://doi.org/10.1016/j.jobe.2020.101367>.
- [29] F. Topak, G.S. Pavlak, M.K. Pekerici, J. Wang, F. Jazizadeh, Collective comfort optimization in multi-occupancy environments by leveraging personal comfort models and thermal distribution patterns, Build. Environ. 239 (2023), 110401, <https://doi.org/10.1016/j.buildenv.2023.110401>.
- [30] C. Xu, et al., A coupled analysis on human thermal comfort and the indoor non-uniform thermal environment through human exergy and CFD model, J. Build. Eng. (2023), 106845, <https://doi.org/10.1016/j.jobe.2023.106845>.
- [31] C. Wang, J. Liu, C.W. Yu, D. Xie, Numerical analysis for the optimization of multi-parameters stratum ventilation and the effect on radon dispersion, J. Build. Eng. 62 (2022), 105375, <https://doi.org/10.1016/j.jobe.2022.105375>.
- [32] N. Serra, Revisiting RANS turbulence modelling used in built-environment CFD simulations, Build. Environ. 237 (2023), 110333, <https://doi.org/10.1016/j.buildenv.2023.110333>.
- [33] B.E. Launder, D.B. Spalding, The numerical computation of turbulent flows, Comput. Methods Appl. Mech. Eng. 3 (2) (1974) 269–289, [https://doi.org/10.1016/0045-7825\(74\)90029-2](https://doi.org/10.1016/0045-7825(74)90029-2).
- [34] J. Abanto, D. Barrero, M. Reggio, B. Ozell, Airflow modelling in a computer room, Build. Environ. 39 (12) (2004) 1393–1402, <https://doi.org/10.1016/j.buildenv.2004.03.011>.
- [35] Y. Zhou, Mengying Wang, Manning Wang, Y. Wang, Predictive accuracy of Boussinesq approximation in opposed mixed convection with a high-temperature heat source inside building, Build. Environ. 144 (2018) 349–356, <https://doi.org/10.1016/j.buildenv.2018.08.043>.
- [36] H. Wang, H. Wang, F. Gao, P. Zhou, Z.( John, Zhai, Literature review on pressure-velocity decoupling algorithms applied to built-environment CFD simulation, Build. Environ. 143 (2018) 671–678, <https://doi.org/10.1016/j.buildenv.2018.07.046>.
- [37] M. Bai, F. Wang, J. Liu, Z. Wang, Experimental and numerical studies of heat and mass transfer performance and design optimization of Fan-coil with high supply chilled water temperature in Air-Conditioning system, Sustain. Energy Technol. Assessments 45 (2021), 101209, <https://doi.org/10.1016/j.seta.2021.101209>.
- [38] ASHRAE, ANSI/ASHRAE Standard 55–2020, Thermal Environmental Conditions for Human Occupancy, Atlanta, Georgia, USA, 2020.
- [39] ISO 7730, Ergonomics of the Thermal Environment-Analytical Determination and Interpretation of Thermal Comfort Using Calculation of the PMV and PPD Indices and Local thermal Comfort Criteria, International Standards Organization, 2005. Accessed: Dec. 23, 2022. [Online]. Available: <https://www.iso.org/standard/39155.html>.